Tellus (1996), 48A, 644–662
Printed in UK – all rights reserved

TELLUS
ISSN 0280–6495

Response of Baltic Sea ice to seasonal, interannual forcing and climate change

By ANDERS OMSTEDT* and LEIF NYBERG, *SMHI, S-601 76 Norrköping, Sweden*

(Manuscript received 12 September 1995; in final form 12 Janaury 1996)

ABSTRACT

The objectives of the present paper are to formulate and explore a coupled sea ice-ocean model and to examine the sensitivity of ice in the Baltic Sea to climate change. The model treats the Baltic Sea as 13 sub-basins with vertical resolution, horizontally coupled by estuarine circulation and vertically coupled to a sea ice model which includes both dynamic and thermodynamic processes. The reducing effect on the barotropic exchange due to sea ice in the entrance area is also added. The model was first verified with data from 3 test periods representing one mild, one normal and one severe ice winter. The maximum seasonal ice extent was then examined on the basis of simulated and observed data for the period 1980–1993. After that, some climate scenarios (both warm and cold) were examined. The seasonal, regional and interannual variations of sea ice were well described by the model, and the thermal response in the Baltic Sea can be realistically simulated applying forcing data from rather few stations. The Baltic Sea system is highly sensitive to climate change, particularly during the winter season. Warming may drastically decrease the number of winters classified as severe, forcing the climate towards more oceanic conditions. On the other hand, cooling will increase the number of severe winters, forcing the climate towards more sub-arctic conditions.

1. Introduction

Knowledge about the energy and water exchange processes between the atmosphere and the sea are of central importance for the understanding of the climate, and also the fact that sea ice is forming in sub-polar and polar seas. The Marginal Ice Zone (MIZ), defined as the area between the minimum and maximum seasonal ice extent, is a large area in which sea ice plays an important role in the energy and water exchange. The role of sea ice in this region is particularly related to changes in energy fluxes, in salt flux and in momentum exchange. Also, river runoff and flow through channels and straits become influenced by sea ice.

The Marginal Ice Zone is probably highly sensitive to climate change, as small variations in, for example, air temperature and wind speed can change the sea from open to ice-covered conditions. The sensitivity of the Marginal Ice Zone to climate change has also been indicated in global climate models (Cubash et al., 1992), however, it is not clear if this sensitivity is due to coarse models or bears any resemblance to observations.

The Baltic Sea is located in the Marginal Ice Zone, Fig. 1, with first year ice forming every year. During the last 100 years the maximum ice extent has ranged from 12 to 100 percent and the length of the ice season from 4 to 7 months (Leppäranta and Seinä, 1985). The seasonal and interannual variations of ice thus are large. Longer historical records on the maximum annual ice extent from the Baltic Sea, dating back at least to 1720, can be found in Seinä and Palosuo (1993).

In the present work, we focus on the response of ice in the Baltic Sea to interannual forcing and

* Corresponding author: Email: aomstedt@smhi.se.

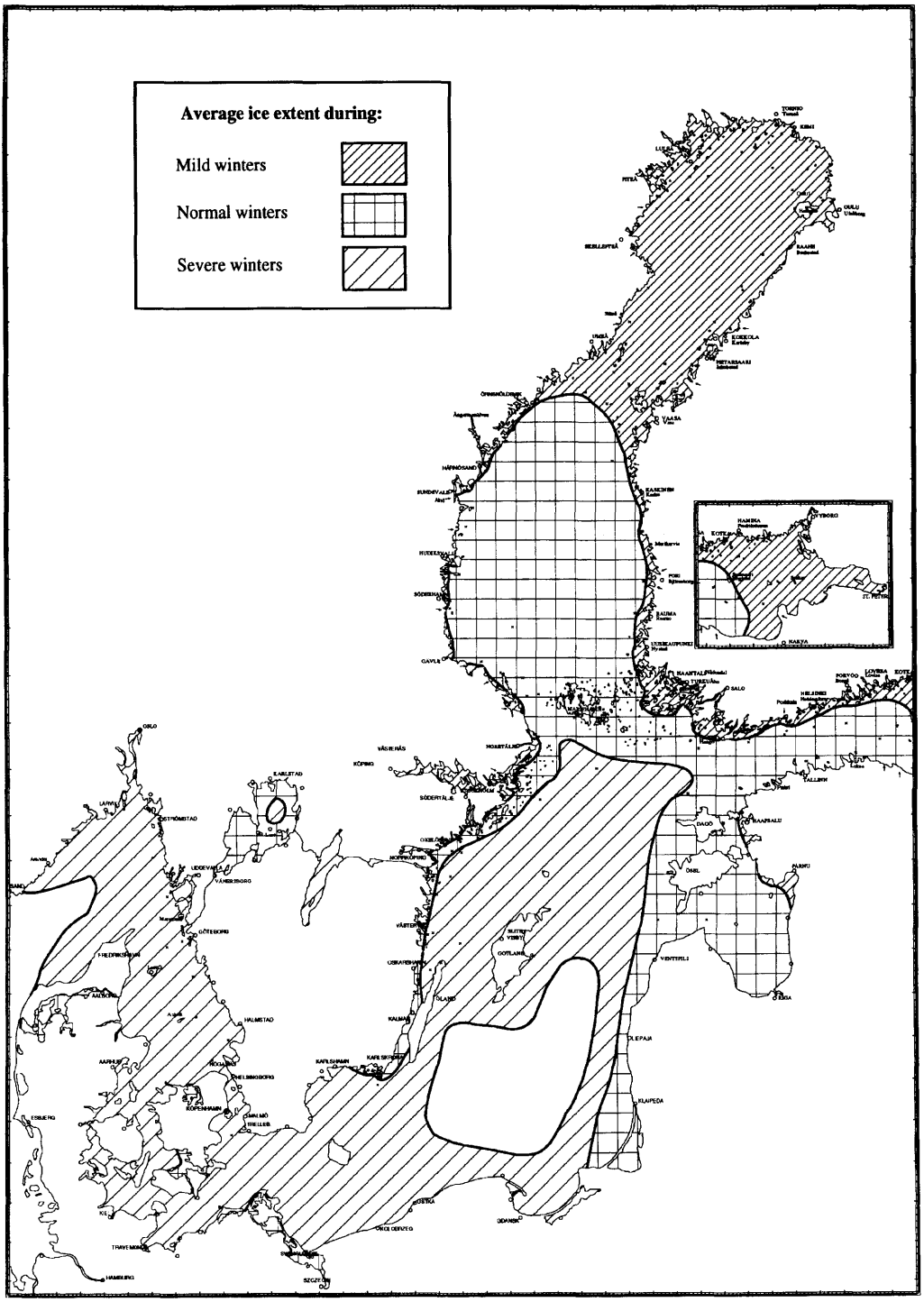

Fig. 1. Average ice extent during mild, normal and severe winters in the Baltic Sea.

to climate change. Within a sea ice climate modelling program for the Baltic Sea, (Haapala et al., 1993), the main philosophy has been first to collect data and select three particular test ice seasons representing mild, normal, and severe ice conditions. The second step is a statistical comparison with the period 1961–1990 and then a consideration of different climate scenarios. We will partly follow these ideas in the present work.

The model by Omstedt (1990 a), in which the Baltic Sea is treated as thirteen coupled sub-basins with vertical resolution, Fig. 2, has in the present work been extended to include sea ice in all sub-basins using the ice model developed by Omstedt (1990b) for semi-enclosed seas. The reducing effect on the barotropic exchange due to sea ice in the entrance area is also added. The modelling of the estuarine circulation has been improved, and observed weather, river runoff and sea level data have been collected for the period 1980–1993 and used as forcing data for the model.

The model was first verified with data for three winters representing a mild winter (1991/92), a normal winter (1983/84) and a severe winter (1986/87). Then the inter-annual variations and the maximum seasonal ice extent were examined. The sea ice sensitivity to climate change was then examined by forcing the model with data from the period 1980–1993 and considering the climate change scenarios for the Nordic countries discussed by Johannesson et al.(1995). The sensitivity to corresponding colder alternatives were also considered. In general the study shows that ice in the Baltic Sea can be well simulated by the present model and that sea ice is very sensitive to interannual variations and to climate change.

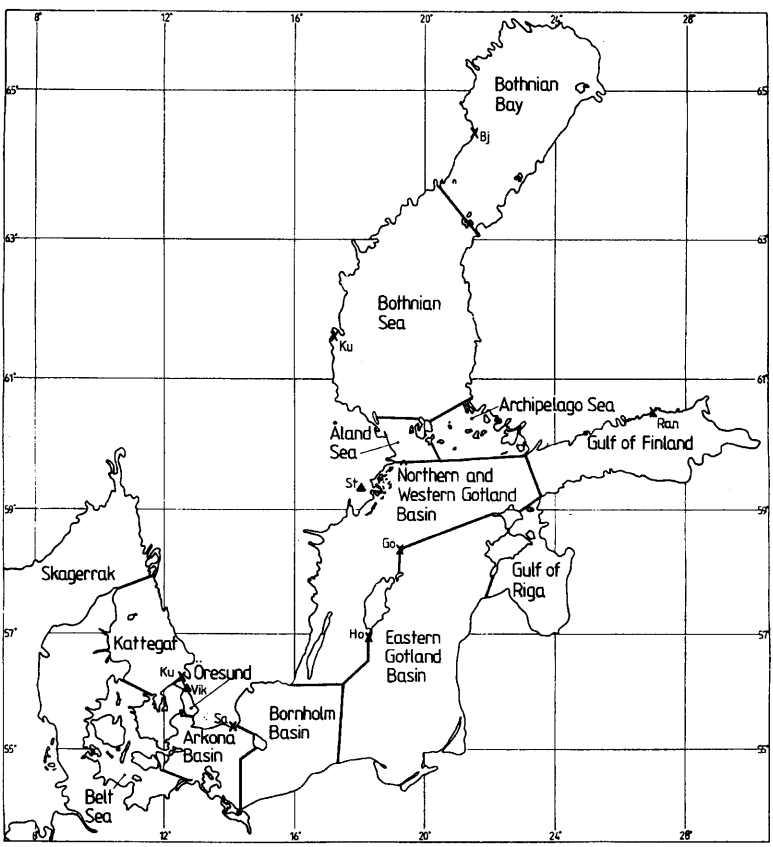

Fig. 2. Division of the Baltic Sea into sub-basins. The crosses indicate the meteorological stations and the triangle the sea level station from which data were extracted in the present study.

In Section 2, the basic model elements are given. Then the forcing data for the period 1980 to 1993 are presented in Section 3. Details of calculations are discussed in Section 4. The results are presented in Section 5. In Section 6, simulations from different climate scenarios are given and climate implications are discussed. Finally, a summary and some conclusions are given in Section 7.

2. Theory

2.1. Introduction

The model divides the Baltic Sea into 13 sub-basins and treats each sub-basin as a system based on the horizontally averaged, time-dependent, advective-diffusive conservation equations of temperature, salinity and momentum and conservation of volume and ice. Turbulent exchange coefficients are calculated from a turbulence model and each sub-basin is coupled to surrounding sub-basins through horizontal flows, Fig. 3. Wall functions are used to parameterize effects of the viscous sublayer at the ice/water interface. The work extends the model by Omstedt (1990a) by including sea ice (Omstedt 1990b), reducing barotropic exchange in the entrance area due to ice and improving the modelling of the estuarine circulation by including a dense bottom current model according to Stigebrandt (1987).

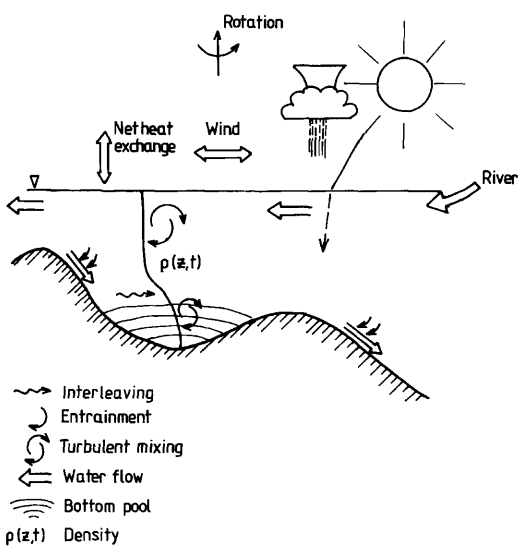

Fig. 3. Model sketch of the ocean model.

2.2. Volume conservation

We first consider conservation of water volume in a freezing sub-basin.

The equation reads:

$$A_s \frac{d\eta}{dt} = Q_{in} - Q_0 + Q_f - \frac{\rho_i}{\rho} Q_{ice}, \quad (1)$$

where t is the time coordinate, η the mean water level, A_s the surface area of the sub-basin, Q_f the river runoff including the net effect of precipitation and evaporation, Q_{in} and Q_0 are the in-and outflows respectively, Q_{ice} is the ice advection out from the sub-basin, ρ_i the ice density and ρ the water density. If ice is not included and we assume a steady state, the volume conservation reads:

$$0 = Q_{in} - Q_0 + Q_f. \quad (2)$$

This equation together with a corresponding equation for the conservation of salinity form the classical theorem by Knudsen (1900) and is often used for the estimation of water budgets in different semi-enclosed basins. In the case of a freezing water body we need to add ice advection.

The mathematical formulation of the in- and outflows require a good understanding of strait dynamics. Geometrical restrictions, stratification and forcing mechanisms are therefore important factors to be considered. In the present formulation of in-and outflows we follow the parametrizations given by Omstedt (1990a) and add effects in the entrance area of the Baltic Sea associated with the reduction of the barotropic flow due to ice. The latter will be discussed in Section 3.

2.3. Strait flows and ice

Ice drift through channels is reduced due to shore ice and ice friction. Ice arching and drift of pack ice through channels will influence the exchange of ice, and friction as well as ice dams will reduce the water exchange. To estimate the importance of sea ice for the in- and outflows through straits one needs to consider some different aspects as: ice drift through the restricted channel, water exchange through the ice-covered channel and changes in water properties due to ice.

Below we will only consider the water exchange

and expand the model developed by Stigebrandt (1992) by including sea ice. Rewriting eqn (1), the volume conservation reads:

$$\frac{A_s d\Delta\eta_e}{dt} = Q_c^i + Q_f - \frac{\rho_i}{\rho} Q_{ice}, \tag{3}$$

where Q_c^i is the in- and outflows through the ice-covered channel and $\Delta\eta_e$ the sea level difference between the ocean and the estuary.

The total sea level drop (η_0–η_e) between the ocean and the estuary is due to the sum of the sea level drop associated with contraction/expansion ($\Delta\eta_c$); the sea level drops associated with bottom friction ($\Delta\eta_f$) and ice friction ($\Delta\eta_f^i$). With simple arguments based upon the different force balances (steady state, etc.) the sea level drops can be written according to:

$$\Delta\eta_c = \frac{U_c^2}{2g}, \tag{4}$$

$$\Delta\eta_f = \frac{U_c^2}{g} \frac{C_d^b L}{(H_c - h_i)}, \tag{5}$$

$$\Delta\eta_f^i = \frac{U_c^2}{g} \frac{C_d^i L}{(H_c - h_i)} N_i^c \left[1 - \frac{U_i}{U_c}\right]^2, \tag{6}$$

$$|\eta_0 - \eta_e| = \Delta\eta_c + \Delta\eta_f + \Delta\eta_f^i, \tag{7}$$

where U_c is the mean speed of the flow in the channel, U_i the mean ice drift, g the gravity constant, C_d^b the bottom friction coefficient, C_d^i the ice friction coefficient, H_c the channel depth, h_i the ice thickness, L the length of the channel and N_i^c the ice concentration in the channel, Fig. 4.

The water flow through the channel reads:

$$Q_c^i = B_m (H_c - h_i) U_c, \tag{8}$$

where B_m is the width of the channel. The ratio between the transport through the strait with (Q_c^i) and without (Q_c) sea ice can now be written according to:

$$\frac{Q_c^i}{Q_c} = \left[1 - \frac{h_i}{H_c}\right]^{3/2} \times \sqrt{\frac{1 + 2C_d^b \frac{L}{H_c}}{1 - \frac{h_i}{H_c} + 2C_d^b \frac{L}{H_c} + 2C_d^i \frac{L}{H_c} N_i^c \left[1 - \frac{U_i}{U_c}\right]^2}}. \tag{9}$$

From eq. (8), one can conclude that for an ice thickness equal to the bottom depth (ice dam), the ratio becomes zero. Also with an ice drift equal to the current speed and with a deep channel compared to the ice thickness, the ratio is equal to 1 (eq. 9). Assuming a completely ice-covered channel with immobile ice and a mean ice thickness much less than the channel depth, one can easily estimate that for a long channel with an ice friction coefficient equal to the bottom friction coefficient, the ratio becomes equal to $\sqrt{0.5}$ or 0.71. The flow through this type of ice-covered channel is thus reduced by 29% compared to the flow through an ice-free channel. In general one can, however, expect that the reducing effect can become even larger, as the interface between ice and water under first year ice is quite rough. Estimates on the ice/water drag coefficient (C_d^i) under first year ice range from $(1–30)\cdot 10^{-3}$, (Shirasawa and Ingram, 1991), which can be compared with a typical water/bottom value (C_d^b) of $3\cdot 10^{-3}$, Table 1.

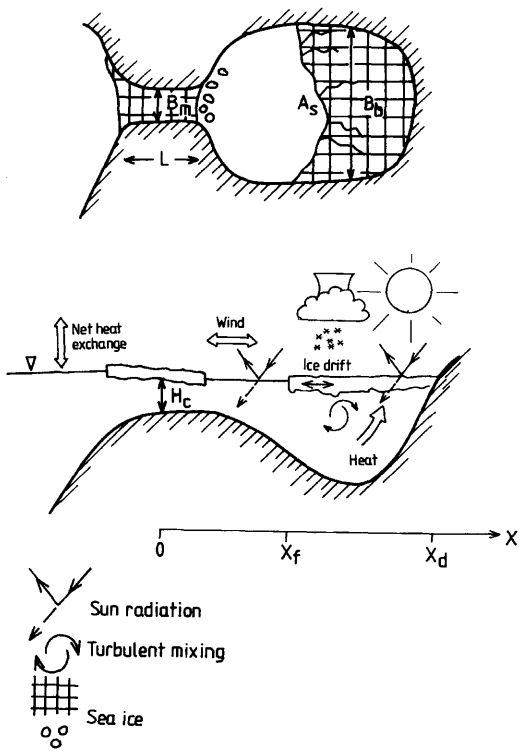

Fig. 4. Model sketch of the ice model.

Table 1. *The parameters and constants in the ice model*

	Constants	Value	Unit
ρ_i	density of ice	910	kg m^{-3}
θ_a	boundary layer angle in air	0	(360)
C_d^i	ice-water drag coefficient	10^{-2}	—
θ_w	boundary layer angle in water	20	(360)
C_d^b	water-bottom drag coefficient	$3\cdot10^{-3}$	—
P_*	strength constant of ice	$2\cdot10^4$	Nm^{-2}
C	reduction constant for opening	20	—
h_s	snow thickness	0.2 h_i	m
k_i	thermal conductivity of ice	2.0	Wm^{-1} K^{-1}
k_s	thermal conductivity of snow	3.0	Wm^{-1} K^{-1}
L_i	latent heat of ice	$3.34\cdot10^5$	J kg^{-1}

2.4. *Heat conservation*

The conservation of temperature for each sub-basin reads:

$$\frac{\partial T}{\partial t}+W\frac{\partial T}{\partial z}=\frac{\partial}{\partial z}\left[\frac{\nu_T}{\mathrm{Pr}_T}\frac{\partial T}{\partial z}\right]+\Gamma_H+\Gamma_{sun}, \qquad (10)$$

where z is the vertical space coordinate positive upwards, T the water temperature, W the vertical mean velocity calculated from the differences between the inflows and outflows, ν_T the kinematic eddy viscosity, Pr_T the turbulent Prandtl number, Γ_H is the sink/source term associated with in- and outflows and Γ_{sun} the source term associated with solar radiation.

In the conservation equations we only deal with friction associated with vertical boundaries, thus the horizontal diffusion terms are not dealt with.

The sink/source term, Γ_H, associated with the in- and outflows to each sub-basin in its finite-difference form, reads:

$$\Gamma_H=\frac{Q_{in}T_{in}}{\Delta V_{in}}-\frac{Q_0 T}{\Delta V_0}, \qquad (11)$$

where T_{in} is the inflow temperature and ΔV_{in} and ΔV_0 are the volumes associated with the in- and outflows respectively.

The source term associated with solar radiation, Γ_{sun}, reads:

$$\Gamma_{sun}=\frac{1}{\rho C_\rho}\{F_{sun}(1-\delta)(1-N_i)+F^i_{sun}N_i\}\,\beta e^{-\beta(D-Z)}, \qquad (12)$$

where F_{sun} and F^i_{sun} are the short wave energy flux to the water and through the ice respectively, N_i ice concentration, C_p specific heat of water, (1-δ) fraction of sun radiation that penetrates into deeper layers, β absorption coefficient and D the total water depth.

The boundary conditions for open water conditions are:

$$\frac{\nu_T}{\mathrm{Pr}_T}\frac{\partial T}{\partial z}=\frac{F_N(t)}{\rho C_p}, \qquad (13)$$

where $F_N(t)$ is the net heat flux to the air/water interface. If bulk formulas are introduced, the net heat flux to the upper layer of the ocean reads:

$$F_N=F_h+F_e+F_{lu}+F_{ld}+\delta F_{sun}+F_{ice}, \qquad (14)$$

where F_h is the sensible heat flux, F_e the latent heat flux, F_{lu} the long-wave radiation upwards, F_{ld} the long-wave radiation downwards, δ fraction of sun radiation that is absorbed in the surface top layer, and F_{ice} the heat flux associated with melting ice that has been advected into the basin. For the parametrization of the fluxes, see Omstedt (1990b) and Elo (1994) for a comparison between different heat flux parametrizations. The heat flux F_{ice} is applied when ice has been advected into the basin or when the upper surface layer has been supercooled. It reads:

$$F_{ice}=\frac{Q_{ice}}{A_s}L\rho_i+\frac{\rho C_p\Delta T\Delta z}{\Delta t}, \qquad (15)$$

where L is the latent heat of ice, ΔT the amount of supercooling in the layer Δz during the time step Δt.

The boundary conditions for ice-covered condi-

tions are:

$$T(z=0)=T_f(S_0), \tag{16}$$

$$\frac{\nu_T}{Pr_T}\frac{\partial T}{\partial z}=\frac{F_w(t)}{\rho C_p}, \tag{17}$$

where T_f is the temperature for freezing, S_0 the interfacial salinity and $F_w(t)$ the heat flux at the ice/water interface. At the ice/water interface we thus assume that both phases are in local equilibrium and utilize the empirical freezing temperature equation (Millero, 1978):

$$T_f=-0.0575\,S_0+1.710523\cdot10^{-3}\,S_0^{3/2}-2.154996\cdot10^{-4}\,S_0^2. \tag{18}$$

The interfacial salinity (S_0) has no obvious value. Rather, it is an outcome of the balance between the melting rate and the turbulent mixing outside the viscous sublayer. The ratio between the interfacial salinity and the far field salinity is not well known. Model studies by Omstedt and Svensson (1992) and by Omstedt and Wettlaufer (1992) illustrated that this ratio could vary from about 0.6 to close to 1. However, in case of melting sea ice and low turbulence (due to, for example, no ice motions) the ratio between interfacial and far field salinity could probably become lower than 0.6. In case of freezing ice the ratio is larger than 1. To bridge the fully turbulent ocean layer beneath the drifting ice and the viscous sublayer adjacent to the ice, wall functions according to Yaglom and Kader (1974) were introduced. These wall functions have also been applied in an operational sea ice model for the Baltic Sea (Omstedt and Nyberg, 1995) and give realistic values on the melting rate of the sea ice. For further discussion see Omstedt (1990b).

2.5. *Salt conservation*

The conservation of salinity in each sub-basin reads:

$$\frac{\partial S}{\partial t}+W\frac{\partial S}{\partial z}=\frac{\partial}{\partial z}\left[\frac{\nu_T}{Sc_T}\frac{\partial S}{\partial z}\right]+\Gamma_S, \tag{19}$$

where Sc_T is the turbulent Schmidt number and Γ_S is the sink/source term associated with in- and outflows. The source/sink term, Γ_S, in its finite-difference form, reads:

$$\Gamma_S=\frac{Q_{in}S_{in}}{\Delta V_{in}}-\frac{Q_0S}{\Delta V_0}-\frac{Q_fS}{\Delta V_s}, \tag{20}$$

where ΔV_s is the surface volume associated with the river runoff.

The boundary condition for open surface conditions are:

$$\frac{\nu_T}{Sc_T}\frac{\partial S}{\partial z}=S_s(E(t)-P(t)), \tag{21}$$

where S_s is the surface salinity and $P(t)$ and $E(t)$ are the evaporation and precipitation fluxes respectively. Zero flux is assumed in the present calculations, although precipitation and evaporation may produce a net fresh water flux.

The boundary condition for ice-covered conditions reads:

$$\frac{\nu_T}{Sc_T}\frac{\partial S}{\partial z}=\frac{\rho_i}{\rho_0}\frac{dh_i}{dt}(S_0-S_i), \tag{22}$$

where ρ_i is the ice density, ρ_0 reference water density, h_i ice thickness and S_i ice salinity.

2.6. *Momentum equations*

The conservation equations for momentum, assuming horizontally homogeneous flow, are solved for each sub-basin. In the Öresund and the Belt Sea, the boundary layer considered is according to a channel flow model with wind stress, while in all other sub-basins, an Ekman flow model is applied.

The momentum equation in the Öresund and the Belt Sea reads:

$$\frac{\partial\rho V}{\partial t}+\frac{W\partial\rho V}{\partial z}=\frac{\partial}{\partial z}\left[\nu_T\frac{\partial\rho V}{\partial z}\right]-\rho g\frac{\partial\zeta}{\partial y}, \tag{23}$$

where V is the mean velocity in the horizontal direction, g the constant of gravity and $\partial\zeta/\partial y$ the sea surface tilt between the Arkona Basin and the Kattegat.

The corresponding equations for the other sub-basins read:

$$\frac{\partial\rho U}{\partial t}+\frac{W\partial\rho U}{\partial z}=\frac{\partial}{\partial z}\left[\nu_T\frac{\partial\rho U}{\partial z}\right]+f\rho V, \tag{24}$$

$$\frac{\partial\rho V}{\partial t}+\frac{W\partial\rho V}{\partial z}=\frac{\partial}{\partial z}\left[\nu_T\frac{\partial\rho V}{\partial z}\right]-f\rho U, \tag{25}$$

where U is the mean velocity in the horizontal direction and f is the Coriolis parameter.

The boundary conditions for open water are:

$$\nu_T \frac{\partial U}{\partial z} = \tau^a_x(t)\rho_0^{-1}, \quad (26)$$

$$\nu_T \frac{\partial V}{\partial z} = \tau^a_y(t)\rho_0^{-1}, \quad (27)$$

where $\tau^a_x(t)$ and $\tau^a_y(t)$ are the wind stresses in the x- and y-directions. The wind stresses are calculated using standard bulk formulation:

$$\tau^a_x = \rho^a C^a_d U^a W^a, \quad (28)$$

$$\tau^a_y = \rho^a C^a_d V^a W^a, \quad (29)$$

where W^a is the wind speed, U^a and V^a are the wind velocity components in the x- and y-directions, and C^a_d is an air drag coefficient.

The boundary conditions for the ice-covered period are:

$$\nu_T \frac{\partial U}{\partial z} = \tau^i_x(t)\rho_0^{-1}, \quad (30)$$

$$\nu_T \frac{\partial V}{\partial z} = \tau^i_y(t)\rho_0^{-1}, \quad (31)$$

where $\tau^i_x(t)$ and $\tau^i_y(t)$ are the ice stresses in the x- and y-directions, which are calculated from:

$$\tau^i_x = \rho_0 C^i_d (U^i - U)|W^i - W^c|, \quad (32)$$

$$\tau^i_y = \rho_0 C^i_d (V^i - V)|W^i - W^c|, \quad (33)$$

where W^i is the ice drift, W^c the current velocity and C^i_d the ice/water drag coefficient.

2.7. *Turbulence model*

The turbulence model used is a buoyancy-extended two-equation model of turbulence; one equation for the turbulent kinetic energy, k, and another for the dissipation rate of turbulent kinetic energy, ε. The turbulence model has been successfully applied by for example Svensson (1979), Omstedt et al. (1983), Omstedt (1987), Leppäranta and Omstedt (1990), Omstedt (1990a, b) and Omstedt et al. (1994) to similar geophysical boundary layers. In a recent paper the model was also compared to other turbulent models (Burchard and Baumert, 1995). The generation of turbulence is calculated from current shear, associated with the wind or the ice drift, and buoyancy production, associated with cooling to the temperature of maximum density or salt rejection due to freezing ice.

The turbulence equations read:

$$\frac{\partial k}{\partial t} + W\frac{\partial k}{\partial z} = \frac{\partial}{\partial z}\left[\frac{\nu_T}{\sigma_k}\frac{\partial k}{\partial z}\right] + P_s + P_b - \varepsilon, \quad (34)$$

$$\frac{\partial \varepsilon}{\partial t} + W\frac{\partial \varepsilon}{\partial z} = \frac{\partial}{\partial z}\left[\frac{\nu_T}{\sigma_\varepsilon}\frac{\partial \varepsilon}{\partial z}\right] + \frac{\varepsilon}{k}(C_{1_\varepsilon}P_s + C_{3_\varepsilon}P_b - C_{2_\varepsilon}\varepsilon), \quad (35)$$

$$P_s = \nu_T\left[\left(\frac{\partial U}{\partial z}\right)^2 + \left(\frac{\partial V}{\partial z}\right)^2\right], \quad (36)$$

$$P_b = \frac{\nu_T g}{\rho_0}\frac{\partial \rho}{\partial z}, \quad (37)$$

$$\nu_T = C_\mu \frac{k^2}{\varepsilon}, \quad (38)$$

where P_s is the production due to shear, P_b is production/destruction due to buoyancy, σ_k and σ_ε are Prandtl/Schmidt numbers, C_μ, C_{1_ε}, C_{2_ε} and C_{3_ε} are constants (Table 2). The surface boundary conditions for turbulent kinetic energy, k, and its dissipation rate, ε, are related to the friction velocity and the buoyancy flux at the air/sea or ice/sea interface. At the lower boundary, a zero flux condition is used.

2.8. *Ice conservation*

In the conservation equation of ice we need to consider both changes in the ice mass due to mechanical and thermodynamic processes (Hibler, 1979). In the present section we concentrate on the thermodynamic part, but also take into account ice ridging and the exchange of ice between the sub-basins. The total ice mass (m_i) in a sub-basin can be estimated as:

$$\frac{m_i}{\rho_i A_s} = N_i(h^c_i + h^r_i) + (1 - N_i)h^f_i, \quad (39)$$

where m_i is the ice mass, N_i the ice concentration, h^c_i the columnar ice thickness, h^f_i the frazil ice thickness (volume per unit area) and h^r_i the equivalent thickness of ridged ice. Within our assumptions the ice conservation equation (derivation of eq. (39)) for each sub-basin reads:

$$\frac{1}{\rho_i A_s}\frac{dm_i}{dt} = N_i\left[\frac{dh^c_i}{dt} + \frac{dh^r_i}{dt}\right] + (1 - N_i)\frac{dh^f_i}{dt} + \frac{Q_{ice}}{A_s}. \quad (40)$$

Table 2. *Model constants in the ocean model (constants within brackets represent values for the Öresund and the Belt Sea)*

	Constant	Value	Unit
C_μ	constant in the turbulence model	0.09	—
$C_{1\varepsilon}$	constant in the turbulence model	1.44	—
$C_{2\varepsilon}$	constant in the turbulence model	1.92	—
$C_{3\varepsilon}$	constant in the turbulence model	0.8	—
β	absorption coefficient	0.3	m^{-1}
δ	fraction of sun radiation	0.4	—
σ_k	Prandtl/Schmidt number	1.4	—
σ_ε	Prandtl/Schmidt number	1.3	—
Pr_T	turbulent Prandt number	1.0	—
Sc_T	turbulent Schmidt number	1.0	—
ρ_a	air density	1.3	kg m^{-3}
ρ_0	reference water density	10^3	kg m^{-3}
C_d^a	air-water drag coefficient	$1.3 \cdot 10^{-3}$	—
k_{min}	minimum kinetic energy	10^{-8} (10^{-6})	$m^2\ s^{-2}$
ε_{min}	minimum dissipation rate	10^{-10} (10^{-8})	$m^2\ s^{-3}$
μ_{min}	minimum turbulent dynamic viscosity	0.01 (0.05)	kg $m^{-1}\ s^{-1}$

The ice growth/decay can be simulated using different models, here we will only consider the basic processes. Columnar ice grows proportionally to the square root of time; in open water, however, the ice grows faster due to the formation of frazil ice which increases linearly with time (cf. Maykut, 1986; Leppäranta, 1983; Omstedt and Svensson, 1984). The rate of columnar and frazil ice growth reads:

$$\rho_i L \frac{dh_i^c}{dt} = \frac{k_i k_s}{k_i h_s + k_s h_i^c}(T_f - T_{sur}) - F_w(t), \tag{41}$$

$$\frac{dh_i^f}{dt} = \frac{F_N}{L\rho_i}, \tag{42}$$

where k_i and k_s are the thermal conductivity of ice and snow respectively, h_s snow thickness and T_{sur} the temperature at the air/ice interface.

The change of the horizontal extent of the ice cover in each sub-basin is assumed to be due to ice drift and thermodynamics (Omstedt, 1990b). The equation reads:

$$\frac{dx_f}{dt} = U_i - \frac{x_f}{h_i}\frac{F_N}{\rho_i L} - U_{adv}\frac{B_m}{B_b}, \tag{43}$$

where x_f is the position of the ice edge (Fig. 4), U_i ice drift, U_{adv} advected ice drift out from the sub-basin, B_m width of the strait and B_b width of the sub-basin. The advected ice drift U_{adv} has a value only when the combined effect of ice drift (U_i) and new frazil ice formation (second term in eq. (43)) is such that the new value of x_f is less than zero. The surplus of ice is then advected out of the basin and x_f is put equal to zero. In the receiving basin the advected ice is used in the heat flux calculation (eq. (15)) or, if ice is already present there, added to the ice in the downstream basin.

The ice drift equation reads:

$$U_i = \begin{cases} U_{free} - \dfrac{P}{x_d - x_f} & \text{on shore winds } U_i \geqslant 0 \\ U_{free} & \text{off shore winds } U_i < 0 \end{cases}, \tag{44}$$

where U_{free} is put equal to 2% of the wind speed and P is the ice strength. In the parametrization of ice strength we follow Hibler (1979) and write:

$$P = P_* h_i\, e^{-C(1-N_i)}, \tag{45}$$

where P_* and C are constants, see Table 1.

The basic assumption is that the ice is deforming for ice drift towards the shore and drifting freely during off-shore drift, see Table 3. The internal compactness of the ice field is allowed to vary between 0.9 and 1, diminishing during off-shore drift. If the compactness rise above 1, compression and ridging occur. This internal compactness is used only to trigger the ridging, so that a reason-

Table 3. *Basic assumptions in the ice model*

Basin	Main ridging direction (360)	Main outflow direction (360)	Comments
The Kattegat	45	340	
The Öresund	45	no	
The Belt	45	no	
The Arkona Basin	0	no	
The Bornholm Basin	0	no	
The E. Gotland Basin	300	no	
The NW Gotland Basin	315	no	
The Gulf of Riga	90	270	
The Gulf of Finland	20	260	
The Archipelago Sea	180	no	reduced ice drift
The Åland Sea	225	no	
The Bothnian Sea	0	180	
The Bothnian Bay	30	210	

able fraction of the ice thickness about mid-winter has been caused by ridging. Note that the ice concentration $N_i=(x_d-x_f)/x_d$, where x_d is the dimension of the sub-basin. For further details see Omstedt (1990b).

3. Forcing data

The meteorological forcing data were observed wind, air temperature, relative humidity and total cloudiness. The data were extracted every 3rd hour from 7 synoptic weather stations (Fig. 2). In the model runs, new data were read in every 3rd hour. The heat fluxes were recalculated every hour, to account for the sun's height above the horizon in a reasonable way. The river runoff data were taken from the SMHI data base (Bergström and Carlsson, 1994) as monthly mean values to each of the sub-basins. The forcing from the open sea was calculated on the basis of daily mean sea level data from the Kattegat (water level station Viken).

The salinity of the inflowing deep water to the Kattegat was prescribed as 32.4 (PSU) and its temperature was set (daily) from a linear interpolation according to mean values for the period 1970–1990 (Juhlin, 1992).

4. Details of calculations

The equations outlined in Section 2 and the continuity equation determining the vertical mean velocities from the in- and outflows form a closed system. The basic model elements were the Baltic Sea model by Omstedt (1990a), in which ice was treated similarly as in the model by Omstedt (1990b) but with ice advection out of each sub- basin added to the model. In the ice model we only assumed one main ridging direction, in the opposite direction the ice was assumed to move freely, see Table 3. The parametrization of the in- and outflows followed Omstedt (1990a). The barotropic flows were forced by observed sea level data in the Kattegat and the total runoff to the Baltic Sea. The baroclinic flows were calculated from the vertical salinity structure in the model assuming geostropic flows. A new baroclinic flow was added to the exchange between the Åland Sea and the Bothnian Sea. The effective sill depth in the northern Åland Sea was assumed to be 90 m. The barotropic exchanges through the Öresund and the Belt Sea were reduced due to ice according to Subsection 2.3. The equation of state followed the UNESCO formula, see Gill (1982).

The inflows were interleaved in the downstream basin at an equal density level. Some inflows were treated as dense bottom currents and mixed with waters above according to the dense bottom current model by Stigebrandt (1987). Dense bottom water mixing was considered in the Arkona Basin, the Eastern Gotland Basin, the Åland Sea and the Bothnian Bay with estimated mean entrainment rates according to Kõuts and Omstedt (1993) and Marmefelt and Omstedt (1993).

The wall functions (the Stanton numbers) for the heat and salt exchange were weighted with the ice concentration giving values for open sea during ice-free conditions and values for ice-covered sea when ice concentrations were equal to 1. Constant ice salinities, about 20% of the typical surface salinity, for each sub-basin were assumed. The snow depth on the ice was assumed to be 20% of the ice thickness, an approximate treatment, because no reliable data were available for forcing the model.

The backbone of the model system is the PROBE code (Svensson, 1986), where in essence, the vertical temperature profile in the water, subject to turbulent mixing etc., is solved. Most of the equations are treated here. Three special subroutines handle the rest: One for water exchange between basins, one for surface heat fluxes, and one for ice. Initial profiles of temperature and salinity for the model were taken from available data around 1 November 1980. The model constants are given in Tables 1, 2. The vertical structure was resolved by a grid with expanding cells from 1 m to 10 m and using up to 100 gridcells in the deep sub-basins. The timestep in the PROBE part of the model was 10 minutes. This was chosen mainly because the coriolis terms in the momentum calculations may lead to poor or diverging results for much longer timesteps. The calculations were then done in 3-h parts, for all basins for a total of 18 time-steps. Results were then written to files and a new 3-h calculation could be started. This arrangment allowed us to stop a run at some prescribed time, examine the results and then continue from the situation reached. This restart facility was very valuable, especially during the early development of the model system. Most ice parameters were calculated every 18th timestep, just before new weather data were applied. Boundary conditions were shifted between ice-covered and open water conditions, at the start of a 3-h period, according to if the mean ice thickness in the basin was more or less than 0.01 m. Salinity was used to evaluate the accuracy of the numerical code. For a time integration of 10 years the vertical mean salinity was in general calculated within ± 0.01 PSU. The model requires about 1 hour CPU-time per one year's simulation on a medium-sized main-frame (VAX 6610).

5. Results

5.1. *Introduction*

In this section, the verification results are presented. Numerically simulated and observed data for the period 1 November, 1980, to 30 September, 1993, will be considered and some different aspects of the results are illustrated in the subsections below.

5.2. *Seasonal and regional variations*

The severe winter 1986/87 was analysed by Omstedt (1990a) using the present modelling approach, but sea ice was, however, not dealt with in that study; instead boundary conditions for an open water surface were applied all through the season, and the simulated temperatures were put equal to the freezing point when they were below freezing. Reasonable results were achieved, but it was clear that sea ice had to be considered in some of the different sub-basins. For example, the sea ice could delay spring warming for more than one month in the Bothnian Bay. In Fig. 5, the calculated and observed data for the Bothnian Bay during the severe winter of 1986/87 are given. Sea ice is now an active component in the model. From the figure one can notice that the ice growth and decay are well captured as well as the water surface temperature and the date for start of spring warming. The corresponding results from the Kattegat are given in Fig. 6.

The observations illustrated in the figures were all taken from sea surface temperature and ice maps at SMHI. These maps summarize available information from several sources and represent integrated information from some days. From the map information horizontally mean values were estimated for each sub-basin.

The model calculations were initialized on 1 November, 1980, no data assimilation was applied, the forcing was only based upon seven synoptic stations, river runoff data and one water level station, and the model assumed horizontal mean properties in each sub-basin. With these model simplifications in mind we regard the results as most encouraging. The regional differences are considerable, which implies that any modelling efforts need to divide the Baltic Sea into several

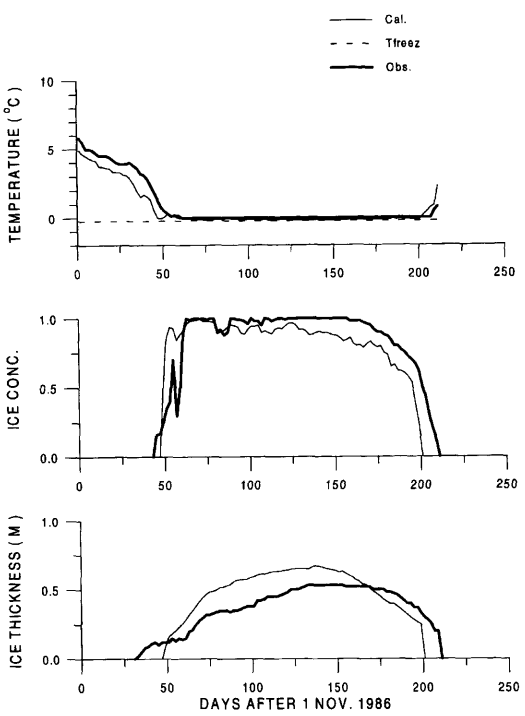

Fig. 5. Observed (thick lines) and calculated (thin lines) data from the Bothnian Bay for the winter 1986/87. The freezing temperature is denoted with a dashed line.

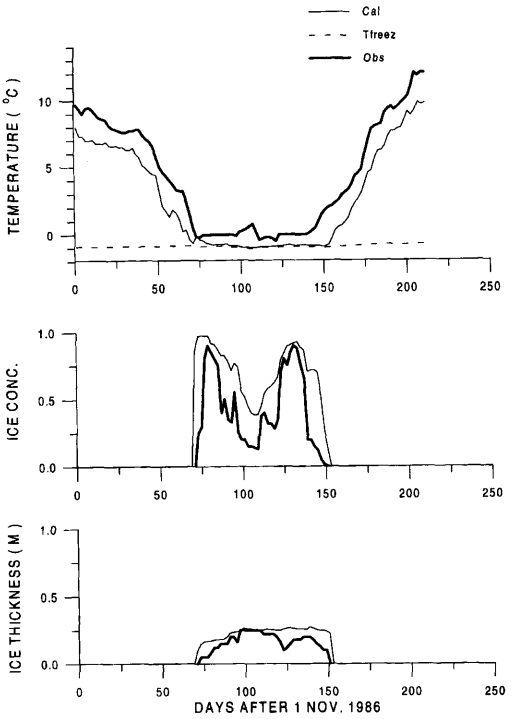

Fig. 6. Observed (thick lines) and calculated (thin lines) data from the Kattegat for the winter 1986/87. The freezing temperature is denoted with a dashed line.

sub-areas. However, the results illustrate that the thermodynamic forcing of the Baltic Sea can be well represented by rather few synoptic weather stations, this is also in accordance with earlier experience (Omstedt, 1990a), and reflects the fact that the thermodynamics of the Baltic Sea is highly forced by the atmosphere and that the dominating weather systems have a much larger scale than the scale of the Baltic Sea sub-basins.

The corresponding results from the other two test ice seasons are presented in Subsection 5.3.

5.3. *Test ice seasons*

Three winters were identified as particular test ice seasons in the joint Baltic Sea Ice Climate Modelling Program (Haapala et al., 1993). These winters represent one mild winter (1991/92), one normal winter (1983/1984) and one severe winter (1986/87). The results from the severe ice winter were presented in Subsection 5.2. In this section we add some results from the normal and mild winters, Figs. 7, 8. A comparison between calculated and observed maximum seasonal ice extent will be given in Section 5.5.

5.4. *Interannual variations*

In Fig. 9 the interannual variations of sea surface temperature, ice concentration and ice thickness from the Bothnian Bay are illustrated. As can be observed, sea ice was simulated each year during the period 1980-1993, but the mean ice thickness and the length of the ice season varied. The corresponding graphs from the Northern and Western Gotland Basin are given in Fig. 10. The winter temperatures give values close to freezing every year, however, the temperature only passes the freezing point during four years. The sea surface temperatures in this figure indicate that the Baltic Sea is most sensitive to climate change;

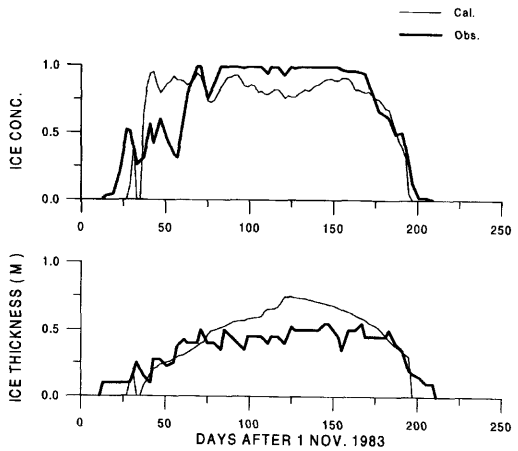

Fig. 7. Observed (thick lines) and calculated (thin lines) data from the Bothnian Bay for the winter 1983/84.

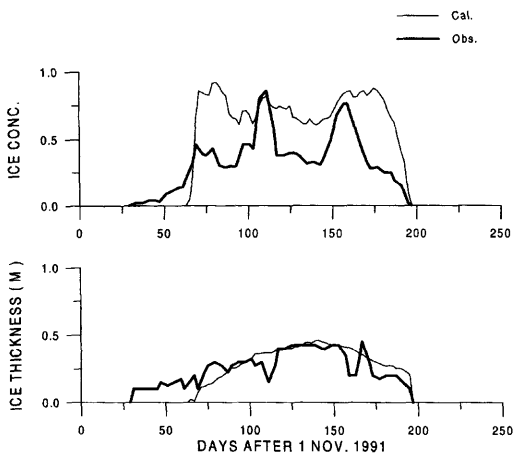

Fig. 8. Observed (thick lines) and calculated (thin lines) data from the Bothnian Bay for the winter 1991/92.

a small change in winter air temperatures will cause large differences in ice extent.

5.5. *Maximum ice extent*

The maximum seasonal ice extent in the Baltic Sea shows large variations. During the studied period it varied from 52,000 to 405,000 km^2, or 12 to 96% of the Baltic Sea surface area, with a mean value for the period of 181,000 km^2 (Seinä and Palosuo, 1993).

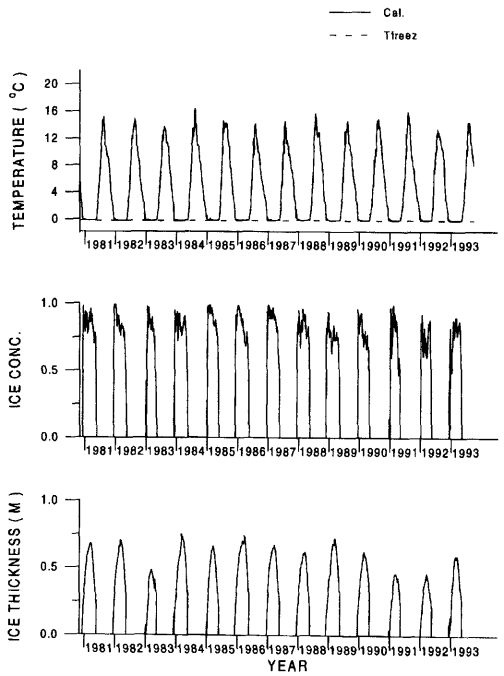

Fig. 9. Simulated interannual variations of surface properties for the Bothnian Bay.

In Fig. 11 and Table 4, simulated and measured maximum ice extent data are given. The mean and root mean square errors in the calculated and the observed maximum ice extent were 18,000 km^2 and 36,000 km^2, respectively. These errors correspond to a mean and a root mean square error of 10% and 20% respectively of the mean ice extent during the studied period. In the table we have listed two alternatives for the date of maximum ice extent. The first one is based upon data from the Finnish Institute of Marine Research (FHI) and the second one from the Swedish Meteorological and Hydrological Institute (SMHI). The mean and the root mean square errors between calculated and observed dates of maximum ice extent were 2 and 13 days respectively on the basis of Finnish data and -2 and 8 days respectively on the basis of Swedish data. The deviation between Finnish and Swedish ice charts for the classification of the date of maximum ice extent reflects the errors in the mapping. In general the model calculations are closer to the data from SMHI, however, the results are satisfactory using both institutes' ice charts, and the model

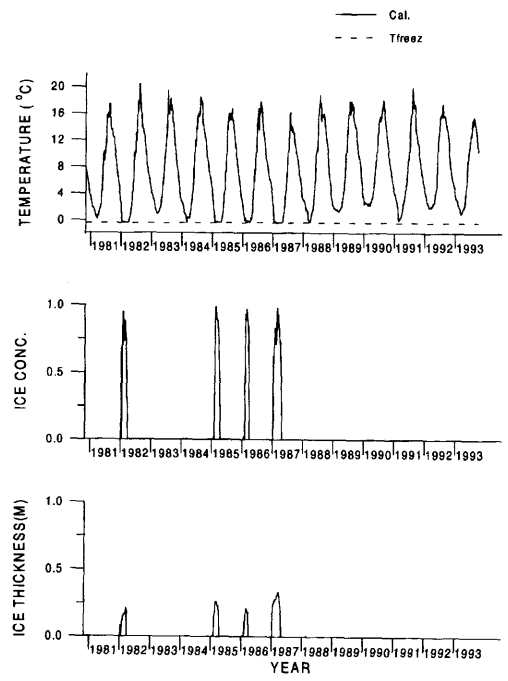

Fig. 10. Simulated interannual variations of surface properties for the Northern and Western Gotland Basin.

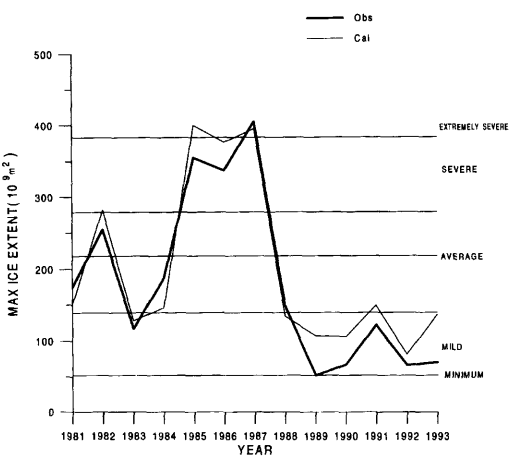

Fig. 11. Observed (thick line) and calculated (thin line) seasonal maximum ice extent for the Baltic Sea.

can in a satisfactory way simulate the maximum seasonal ice extent during very different winter conditions.

6. Climate implications

6.1. Introduction

During the late 20th century, scientists have become more and more concerned about man's influence on climate. Scientists agree that due to the increasing atmospheric concentration of greenhouse gases the atmosphere will become warmer. On the other hand, anthropogenic emissions of aerosols will cool the atmosphere. In a recent assessment of the climate of Europe (Schuurmans et al., 1995), the observed trends during the 20th century as well as recent model results were reviewed. In general, almost all stations across Europe have indicated warming during the present century. The warming anomaly for the period 1981–1990, compared with that for 1951–1980 indicates an increased temperature over the Baltic Sea of about 0.25°C, (Parker et al., 1994). But whether this is an effect of increased concentrations of greenhouse gases or natural variability in the climate system is not clear. To address the question about climate change, several model efforts are now going on. In general control runs with the present-day concentrations of greenhouse gases are first run using global models. Then, experiments with increased concentration of greenhouse gases are run. Results from these runs with a CO_2 doubling, i.e. around 2030 under a business-as usual emission scenario, indicate considerable warming with large regional differences, (Schuurmans et al., 1995).

Coupled atmospheric — oceanic models have also revealed the existence of more than one steady state solution. Manabe and Stouffer (1988) illustrated the existence of at least two stable steady state solutions, the first corresponding to the circulation system we observe today with deep water formation in the North Atlantic and with an estuarine circulation that brings warm and saline water northward. In the second steady state solution, the North Atlantic deep water formation is not present, showing a much colder and fresher North Atlantic, which would drastically cool its surrounding lands (Broecker, 1995) and the Baltic Sea.

The present implications of climate change increases the need to understand the sensitivity of the different energy and water cycle loops in the climate system. In the present section we adress

Table 4. *Observed and numerically simulated maximum seasonal ice extent (ME = Mean error, RMSE = root mean square error)*

Observed data				Modelled data			Model errors		
	date							date	
year	FHI	SMHI	max ice extent (10^3 km^2)	year	date	max ice extent (10^3 km^2)	max ice (10^3 km^2)	FHI (days)	SMHI (days)
1981	0317	0316	175	1981	0307	151	−24	−10	−9
1982	0223	0226	255	1982	0226	282	27	3	0
1983	0303	0312	117	1983	0313	128	11	10	1
1984	0323	0322	187	1984	0327	146	−41	4	5
1985	0222	0221	355	1985	0220	400	45	−2	−1
1986	0302	0227	337	1986	0301	376	39	−1	2
1987	0316	0313	405	1987	0306	395	−10	−10	−7
1988	0319	0319	149	1988	0225	134	−15	−23	−23
1989	0119	0227	52	1989	0223	107	55	35	−4
1990	0118	0131	67	1990	0129	106	39	11	−2
1991	0220	0219	122	1991	0219	149	27	−1	0
1992	0221	0220	66	1992	0222	81	15	1	2
1993	0225	0224	70	1993	0304	136	66	7	8
							ME = 18 RMSE = 36	ME = 2 RMSE = 13	ME = −2 RMSE = 8

the question of the sensitivity of ice in the Baltic Sea to climate change.

6.2. *Maximum seasonal ice extent*

From statistical studies based upon long time series, Seinä (1993) has shown a high correlation between the maximum seasonal ice extent and the air temperatures in Stockholm or Helsinki. Based upon a linear relation between maximum ice extent (30-years running average) and air temperatures, Seinä (1993) predicted changes due to global warming. The change in maximum ice extent was estimated from −720 km^2/year to −5920 km^2/year for an increasing air temperature of 0.2 to 0.8°C per decade.

In a recent study of climate change scenarios for the Nordic Countries (Johannesson et al., 1995), the temperature change for the Baltic Sea was estimated to an increase in winter and summer air temperatures equal to 0.55 and 0.25°C per decade, respectively, (annual mean 0.4°C) from a 1961–1990 baseline with a sinusoidal variation between the summer and winter values. By running the present model with the same forcing data as before (period 1980–1993) but increasing the air temperature according to the above scenario, two warming experiments were run, one corresponding to a 50 years' warming (Warm 1) and the other a 100 years' warming (Warm 2), Fig. 12. As can been seen in the figure climate warming will drastically reduce the ice extent, particularly during years which were classified as severe and

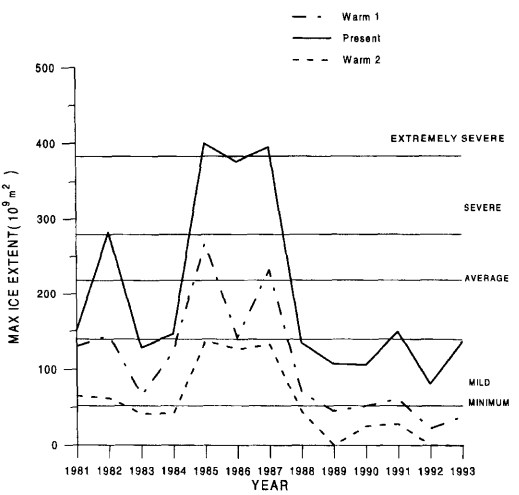

Fig. 12. Simulated seasonal maximum ice extent for a warmer climate.

extremely severe winters. The mean decrease of the ice extent during the period was calculated to 92,000 km^2 and 145,000 km^2 for the 50 and 100 years' climate change case. This is within the best guess scenarios by Seinä (1993) corresponding to an increased temperature of 0.4°C per decade (−72,000 to −148,000 km^2 and −144,000 to −296,000 km^2 for the 50 and 100 years' climate change scenario). It should, also, be noted that the reduction in maximum ice extent is not linearly related to the air temperature in the present model results as was a basic assumption in the statistical model by Seinä (1993). This is also what one should expect as there are several non-linear processes involved in the dynamics and thermodynamics. Ocean mixing, which controls the cooling rate, is for example, related to the cube of the wind during deepening of the thermocline, and long wave radiation, which is important for the energy loss is related to the 4th power of the air temperature. For the maximum ice extent one thus need to consider both dynamic and thermodynamic processes. This was also illustrated by Omstedt and Nyberg (1995) for the normal ice winter of 1993/94, when the maximum ice extent was due partly to ice formation and partly to ice drift.

In Fig. 13, the two corresponding cold climate scenarios are illustrated. As global warming is believed to be the most probable climate scenario, most studies neglect to study a colder alternative.

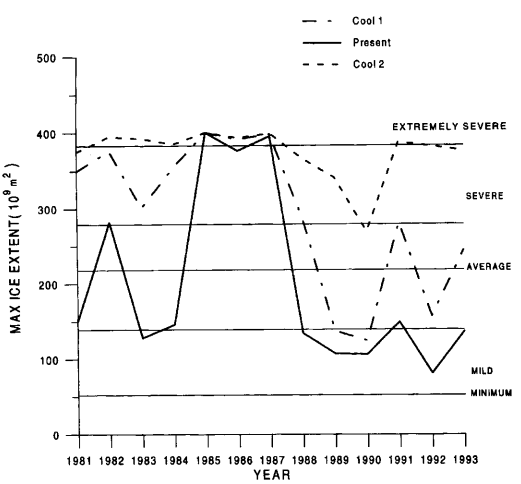

Fig. 13. Simulated seasonal maximum ice extent for a colder climate.

However, for the understanding of the sensitivity of each climate sub-system, it is of importance to consider also colder alternatives. Here we have considered a decreased air temperature of −0.4°C per decade and one 50 (Cool 1) and one 100 years' cold scenario (Cool 2). The maximum ice extent is most sensitive to colder temperatures and the number of years with severe ice conditions is drastically increased. The mean decrease or increase in ice extent for the different scenarios are summarized in Table 5.

From the simulations we can conclude that the Baltic Sea ice shows large interannual variation and is very sensitive to climate change. Warming will force the Baltic Sea climate towards oceanic conditions, while cooling will force the system toward sub-arctic conditions.

6.3. *Maximum ice thickness and length of ice season*

The simplest way to detect climate change in the ocean is probably to observe changes in the thickness of fast ice. This should also be true for the length of the ice season, defined as the number of days with ice. On the basis of a statistical analysis with data from the Baltic Sea, Leppäranta and Seinä (1985) showed that the length of the ice season had decreased 20–30 days per century. Empirical relations and simple analytical models have successfully related level ice thickness to air temperatures. For example, Billelo (1980) showed from weekly measurements of fast ice thicknesses in Canada and Alaska, that the decay was almost linear with time. On the basis of simple analytical models Leppäranta (1993) showed that with an increasing air temperature of 1°C one should expect a 0.1 m thinner ice and a 14 days shorter ice season in the Baltic Sea. The corresponding

Table 5. *Calculated mean change ($\Delta\bar{A}_i$) (period 1980–1993) and mean maximum ice extent ($\bar{A}_i$) in the Baltic Sea for the different climate scenarios*

Scenarios	$\bar{A}_i$ (10^3 km^2)	$\Delta\bar{A}_i$ (10^3 km^2)
present	199	
Warm 1	107	−92
Warm 2	54	−145
Cool 1	292	+93
Cool 2	374	+175

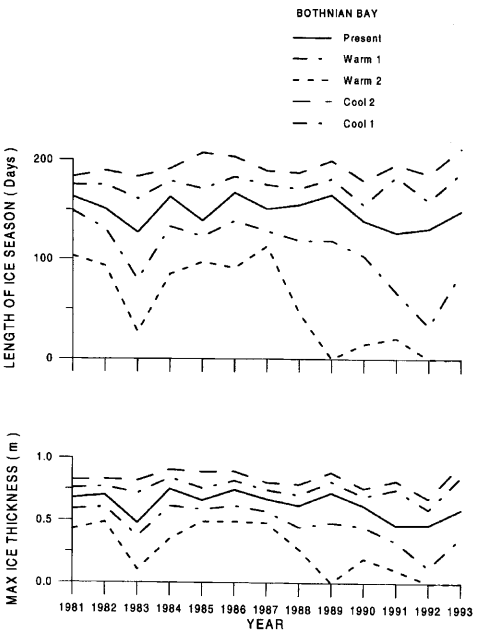

Fig. 14. Simulated maximum ice thickness and length of ice season for the Bothnian Bay.

predictions in the present study are illustrated for the Bothnian Bay in Fig. 14. It should be noticed that in the present paper we consider sea ice and that the seasonal maximum ice thickness includes both level and ridged ice. The mean maximum ice thickness and mean number of days with ice for the 1980–1993 period in the Bothnian Bay, were calculated to 0.63 m and 148 days, respectively. For the warming scenarios 1 and 2 the ice thickness decreased by 0.16 and 0.37 m, respectively. The corresponding reduction in ice season was 40 and 95 days, respectively. In the case of the Gulf of Finland the mean maximum ice thickness and mean number of days with ice were 0.48 m and 105 days, respectively. The change for the different scenarios are given in Table 6. Again we can notice that no simple linear relation holds and that large interannual variations in the reduction are predicted.

6.4. Ice in straits

In any climate models for the Baltic Sea, special efforts need to be paid to the strait flow dynamics in the entrance area. For ice-free conditions, the barotropic model developed by Stigebrandt (1980) and applied in the present model gives a reasonably accurate desciption of the in- and outflows to the Baltic Sea (the explained variance between calculated and observed water levels from Stockholm, representing the mean sea level of the Baltic Sea, was for the studied period equal to 0.77). If sea ice is present in the Baltic Sea entrance area, one also needs to add the effects of ice, particularly when colder scenarios are considered. In Subsection 2.3 we therefore developed a model on how the flow is reduced due to ice. In the theory we only consider increased friction and decreased cross sections in the Öresund and the Belt Sea. Effects of changing sea levels in the ocean due to thermal expansion or changes in the global distribution of freshwater also need to be considered. If such information is available this could easily be added to the barotropic model. However, this has not been dealt with in the present work.

Table 6. *Mean change in number of ice days and maximum ice thickness for the Bothnian Bay and the Gulf of Finland for the different climate scenarios*

Scenarios	Bothnian Bay		Gulf of Finland	
	ice days (Days)	max iceth. (m)	ice days (Days)	max iceth. (m)
present	148	0.63	105	0.48
Warm 1	−40	−0.16	−58	−0.21
Warm 2	−95	−0.37	−83	−0.36
Cool 1	+25	+0.12	+35	+0.13
Cool 2	+44	+0.20	+57	+0.24

To reflect climate change we have only considered changes in the air temperature in the present study. For future work we need to force the model with consistent specifications of possible climate developments, including consistent changes in wind, weather, river runoff and inflows. This can probably only be achieved by using outputs from global circulation models.

7. Summary and conclusions

The main objective of the present study was to examine the sensitivity of ice in the Baltic Sea to climate change. The model by Omstedt (1990a), in which the Baltic Sea is treated as thirteen

horizontally coupled sub-basins with vertical resolution, was extended to include sea ice in all sub-basins using the coupled ice-ocean model by Omstedt (1990b). Some other improvements were also added to the model: one model for the reduction of the barotropic flow in the entrance of the Baltic Sea due to ice, and one model for the dense bottom currents according to Stigebrandt (1987).

On the basis of weather, river runoff and sea level data the model was run during the period 1980–1993. The model was first verified with data from three test periods representing one mild, one normal and one severe ice winter. The maximum seasonal ice extent was then examined on the basis of simulated and observed data. The sea ice sensitivity to climate change — both warm and cold scenarios — was finally examined.

The conclusions from the paper are summarized as follows.

(1) The seasonal and interannual, as well as regional, variations of surface temperatures and ice in the Baltic Sea are well described by the present model.
(2) The thermal response including sea ice can be numerically simulated in a realistic way, applying forcing data from rather few weather stations.
(3) The Baltic Sea is a system highly sensitive to climate change, particularly during the winter season. Warming may drastically decrease the number of winters classified as severe, forcing the climate towards oceanic conditions. On the other hand, cooling will increase the number of winters classified as severe and forcing the climate towards sub-arctic conditions.
(4) Both dynamic and thermodynamic processes need to be considered in the ice-ocean modelling effort as several non-linear processes are important. Simple statistical or analytical solutions give insight in the problem considered, but only for some part of the problem.
(5) Reliable climate predictions will need consistent specifications of forcing data, including wind, weather, river runoff and inflows.

8. Acknowledgements

This work has been financed by SMHI and the Swedish Natural Science Research Council (contract G-GU 09151–306 and –307). Special thanks are given to Ari Seinä for providing the data on the maximum seasonal ice extent, to Bengt Carlsson for river runoff data, to Barry Broman for water level data and to Stig Nilsson for ice data. Bertil Håkansson and two anonymous reviewers made some valuable comments on an earlier draft. Also the drawing by Eva-Lena Ljungqvist and the printing by Gunilla Mild are gratefully acknowledged.

REFERENCES

Bergström, S. and B., Carlsson, 1994. River runoff to the Baltic Sea: 1950–1990. *Ambio*, **23**, 280–287.

Billelo, M. A. 1980. Decay pattern of fast sea ice in Canada and Alaska. In *Sea ice processes and models*, edited by R. S. Pritchard,pp. 313–326. University of Washington Press, Seattle, USA.

Broecker, W. S. 1995. Chaotic climate. *Scientific American* **273**, 44–50, November.

Buchard, H. and H. Baumert, 1995. On the performance of a mixed-layer model based on the k-ε turbulence closure. *J. Geophys. Res.* **100**, C5, 8523–8540.

Cubash, U., Hasselmann, K., Höck, H., Maier-Reimer, E., Mikolajewicz, U., Santer, B. D. and R., Sausen, 1992. Time-dependent greenhouse warming computations with a coupled ocean-atmosphere model. *Climate Dynamics* **8**, 55–69.

Elo, A-R. 1994. A sensitivity analysis of a temperature model of a lake examining components of the heat balance. *Geophysica* **30**, 1–2, 79–92.

Gill, A. E. 1982. *Atmosphere-ocean dynamics. International Geophysical Series* **30**, Academic Press, New York, USA.

Haapala, J., Leppäranta, M. and Omstedt, A. 1993. Forcing data for the Baltic Sea ice climate modelling. *Proc. 1st Workshop on the Baltic Sea ice climate*, Tvärminne, Finland 24–26 August, 1993. Report Series in Geophysics, 27, University of Helsinki, Department of Geophysics, 95–107.

Hibler III, W. D. 1979. A dynamic thermodynamic sea ice model. *J. Phys. Oceanogr.* **9**, 815–846.

Johannesson, T., Jonsson, T., Källen, E., Kaas, E. 1995. Climate change scenarios for the Nordic Countries. *Climate Research* **5**, 181–195.

Juhlin, B. 1992. 20 years measurements along the Swed-

ish coast performed by the Coast Guard. (In swedish). *SMHI Reports Oceanografi* **54**, 1–67. SMHI, S-601 76 Norrköping, Sweden.

Knudsen, M. 1900. Ein hydrographischer Lehrsatz. *Ann. der Hydrographie und Maritimen Met.*, 316–320.

Kõuts, T. and A., Omstedt, 1993. Deep water exchange in the Baltic Proper. *Tellus* **45A**, 311–324.

Leppäranta, M. 1983. A growth model for black ice, snow ice and snow thickness in subarctic basins. *Nordic Hydrology*, 59–70.

Leppäranta, M. 1993. The Baltic Sea ice climate: An introduction. *Proc. 1st Workshop on the Baltic Sea ice climate,* Tvärminne, Finland, 24–26 august 1993. Report Series in Geophysics, 27, University of Helsinki, Department of Geophysics, 5–17.

Leppäranta, M. and A., Seinä, 1985. Freezing, maximum annual ice thickness and breakup of ice on the finnish coast during 1930–1984. *Geophysica* **21**, 87–104.

Leppäranta, M. and A., Omstedt, 1990. Dynamic coupling of sea ice and water for an ice field with free boundaries. *Tellus* **42A**, 482–495.

Manabe, S. and R. J. Stouffer, 1988. Two stable equilibria of a coupled ocean–atmosphere model. *J. of Climate* **1**, 841–866.

Marmefelt, E. and A., Omstedt, 1993. Deep water properties in the Gulf of Bothnia. *Continental Shelf Research,* vol. **13**, no. 2/3, 169–187.

Maykut, G. A. 1986. The surface heat and mass balance. In: *The geophysics of sea ice* (ed. N. Untersteiner). The NATO ASI Series, B146. Plenum: USA, 395–463.

Millero, F. J. 1978. Freezing point of sea water. 8th report of the Joint Panel on Oceanographic Tables and Standards. *UNESCO Tech. Paper Mar. Sci.* **28** (annex 6). UNESCO, Paris, France.

Omstedt, A. 1987. Water cooling in the entrance of the Baltic Sea. *Tellus* **39A**, 254–265.

Omstedt, A. 1990a. Modelling the Baltic Sea as thirteen sub-basins with vertical resolution. *Tellus* **42A**, 286–301.

Omstedt, A. 1990b. A coupled one-dimensional sea ice-ocean model applied to a semi-enclosed basin. *Tellus* **42A**, 568–582.

Omstedt, A. and U., Svensson, 1984. Modelling supercooling and ice formation in a turbulent Ekman layer. *J. Geophys. Res.* **89**, C1, 735–744.

Omstedt, A. and U. Svensson, 1992. On the melt rate of drifting ice heated from below. *Cold Regions Science and Tech.* **21**, 91–100.

Omstedt, A. and J. S. Wettlaufer. Ice growth and oceanic heatflux. Models and measurements. *J. Geophys. Res.* **90** C5, 9029–9049.

Omstedt, A. and L., Nyberg, 1995. A coupled ice-ocean model supporting winter navigation in the Baltic Sea. Part 2: Thermodynamics and meteorological coupling. *SMHI Reports,* RO 21. SMHI, S-601 76 Norrköping, Sweden.

Omstedt, A., Sahlberg, J. and U. Svensson, 1983. Measured and numerically simulated autumn cooling in the Bay of Bothnia. *Tellus* **35A**, 231–240.

Omstedt, A., Carmack, E. C. and R. W., McDonald, 1994. Modelling the seasonal cycle of salinity in the Mackenzie shelf/estuary. *J. Geophys. Res.* **99**, C5, 10011–10021.

Parker, D. E., Jones, P. D., Folland, C. K. and Bevan, A., 1994. Interdecadal changes of surface temperature since the late nineteenth century. *J. Geophys. Res.* **99**, D7, 14373–14399.

Schuurmans, C, Cattle, H., Choisnel, E., Dahlström,B., Gagaoudaki, C., Jorgensen, A,M., Muller-Westermeier,G. and Orfila, B., 1995. *Climate of Europe. Recent variation, present state and future prospects.* First Europa Climate assessment. ECSN, 1995. ISBN 90–369–2069–8. Royal Netherlands Meteorological Institute, the Netherlands.

Seinä, A. 1993. Ice time series of the Baltic Sea. *Proc. 1st Workshop on the Baltic Sea ice climate*, Tvärminne, Finland, 24–26 august 1993. Report Series in Geophysics, 27, University of Helsinki, Department of Geophysics, 87–90.

Seinä, A. and E. Palosuo, 1993. The index of maximum annual extent of ice cover in the Baltic Sea 1720–1992 (In Finnish). *Meri* **20**. Finnish Institute of Marine Research, Helsinki, Finland.

Shirasawa, K. and R. G. Ingram, 1991. Characteristics of the turbulent ocean boundary layer under sea ice. Part: 1 A review of the ice-ocean boundary layer. *J. Marine Systems* **2**, 153–160.

Stigebrandt, A. 1980. Barotropic and baroclinic response of a semi-enclosed basin to barotropic forcing from the sea. In: *Fjord oceanography* (eds. H. J. Freeland, D. M. Farmer and C. D. Levings). Plenum, New York, USA, 141–164.

Stigebrandt, A. 1987. A model for the vertical circulation of the Baltic deep water. *J. Phys. Oceanogr.* **17**, 1772–1785.

Stigebrandt, A. 1992. Bridge-induced flow reduction in sea straits with reference to effects of a planned bridge across Öresund. *Ambio* **21**, 130–134.

Svensson, U. 1979. The structure of the turbulent Ekman layer. *Tellus* **31**, 340–350.

Svensson, U. 1986. PROBE–An instruction manual. *SMHI Report Oceanography,* no. 10, SMHI, S-601 76 Norrköping, Sweden, 90 pp.

Yaglom, A. M. amd Kader, B. A. 1974. Heat and mass transfer between a rough wall and turbulent fluid flow at high Reynolds and Peclet numbers. *J. Fluid Mech.* **62**, 601–623.